Climate Dynamics (2005) 25: 1–17
DOI 10.1007/s00382-004-0483-0

Edvin Aldrian · Dmitry Sein · Daniela Jacob
Lydia Dümenil Gates · Ralf Podzun

Modelling Indonesian rainfall with a coupled regional model

Received: 11 May 2004 / Accepted: 16 September 2004 / Published online: 14 May 2005

Abstract Long-term high-resolution coupled climate model simulations using the Max Planck Institute Regional Climate Model and the Max Planck Institute Ocean Model have been performed with boundary forcings from two reanalyses: firstly from the European Centre for Medium-Range Weather Forecasts, and secondly from the joint reanalysis of the National Centers for Environmental Prediction and the National Center for Atmospheric Research. This study employs a special coupling setup using a regional atmospheric model and a global ocean model. The latter model applies a special conformal grid from a bipolar orthogonal spherical coordinate system, which allows irregular positions of the poles and focuses on the detail over the Maritime Continent. The coupled model was able to simulate stable and realistic rainfall variabilities without flux correction and at two different ocean resolutions. The coupled system is integrated for a period between 1979 and 1993 and the results are then compared to those from uncoupled runs and from observation. The results show improved performance after coupling: a remarkable reduction of overestimated rainfall over the sea for the atmospheric model and of warm SST biases for the ocean model. There is no significant change in rainfall variability at higher ocean model resolution, but the ocean circulation shows less transport variability within the Makassar Strait in comparison to observations.

This paper has not been published or considered by any other journal in any language.

E. Aldrian · D. Sein · D. Jacob · L. D. Gates · R. Podzun
Max Planck Institut für Meteorologie,
Bundesstraße 55, 20146 Hamburg, Germany

E. Aldrian (✉)
Agency for the Assessment and Application of Technology,
BPPT, Jakarta, Indonesia
E-mail: edvin@bppt.go.id
Tel.: +49-40-41173313
Fax: +49-40-41173391

L. D. Gates
National Science Foundation, 4201 Wilson Blvd,
Arlington, VA 22230, USA

1 Introduction

The maritime continent, Indonesia, is the largest archipelago and mostly covered by ocean. Study concerning the temporal and spatial variation of rainfall of Indonesia using a regional climate model (RCM) has been reported by Aldrian et al. (2004). One problem in simulating rainfall of the region is the appropriate land–sea representation (Aldrian et al. 2003). The area is highly complex with large ocean coverage and chains of islands. Intense ocean atmosphere interactions take place at the ocean surface in this most convective region of the world. Due to large ocean areas, such processes will be important in modeling the climate of the region, because the local sea surface temperature (SST) is among the major factors that drive rainfall variability across the Maritime Continent (e.g., Nicholls 1979; Hackert and Hastenrath 1986; Hendon 2003; Aldrian and Susanto 2003). With a stand alone (uncoupled) atmospheric or ocean model, such processes cannot be simulated adequately. The uncoupled atmospheric model uses the spatially and temporally prescribed and interpolated SST, while the uncoupled ocean model uses the ocean surface fluxes calculated using empirical formulae. Such configurations disregard dynamical interactions that occur at the ocean surface. An integrated or coupled ocean/atmosphere model gives more realistic dynamics close to the ocean surface, where ocean atmospheric exchanges take place at higher frequency determined by the coupling setup. Regional climate studies using a coupled ocean/atmosphere model for the maritime continent are relatively new.

Our approach is to use a high-resolution, regional atmospheric model coupled to an ocean model with an

adjusted special conformal grid that both have a comparable high-resolution in the region. The coupled system will provide high-resolution regional interpretations of large-scale modeling. A nested RCM could downscale global circulation model (GCM) results to a regional scale. The Max Planck Institute (MPI) RCM or REMO (Jacob 2001; Jacob et al. 2001) is suitable for this purpose, because REMO provides detailed forecasts of weather parameters close to the ground and an improved simulation of clouds and rainfall compared to a GCM. REMO has been coupled with a regional ocean model HAMburg Shelf Ocean Model (HAMSOM) over Baltic seas (Schrum et al. 2003), while there is no REMO model coupled experiment with an Ocean Global Circulation Model (OGCM) yet. On the other hand, the MPI OGCM, the MPI-OM1 (Marsland et al. 2003) can also be used for a regional climate study (Marsland and Wolff 1998, 2001) . MPI-OM1 is the latest development of the Hamburg Ocean Primitive Equation (HOPE) ocean model (Wolff et al. 1997). A major improvement is the transition from a staggered E-grid to an orthogonal curvilinear Arakawa C-grid (Arakawa and Lamb 1977) and arbitrary placement of the poles from a bipolar orthogonal spherical coordinate system. This coupling method, to the authors' knowledge, is relatively new to the region.

The purposes of this paper are: to analyze the performance of a very high resolution coupled-climate model; to compare the result with observations; and to study the implication of coupling to atmosphere and ocean and to see the importance of different ocean model resolutions and model boundary forcings. Due to limited observation data, emphasis will be given to parameters whose observation data are available, i.e. rainfall, SST and ocean current from the monthly to the interannual time scale. The period of analyses is from 1979 to 1993. The outline of this paper is as follows: Sect. 2 presents the data and model setup, Sect. 3 discusses the implication of coupling for the atmosphere and Sect. 4 the implication for the ocean. Finally, Sect. 5 summarizes the highlights of the findings.

2 Data and model setup

2.1 Data

The data used in this study are monthly rainfall data collected by the Indonesian Meteorological and Geophysical Agency (BMG) at 167 stations all over Indonesia, and monthly mean rainfall data from the WMO-NOAA project on The Global Historical Climatology Network (GHCN; Vose et al. 1992) from 1979 to 1993. For the area of this study (19°S–8°N and 95°E–145°E), there are 545 rain gauges. They are referred hereafter as the "rain gauge" data. The data has passed some quality control tests including the homogeneity test before they are incorporated into GHCN (Peterson et al. 1998). These data are gridded to match the REMO 0.5° resolutions using the Cressman (1959) method. As the second observation data set, a combination of gauge observations with satellite estimates from the Global Precipitation Climatology Project (GPCP; Huffman et al. 1997) at the 1° spatial resolution is used. The second data set provides more reliable ocean rainfall data than land rain gauge interpolated data into the ocean. The data has been interpolated into the REMO grid as well.

This study uses surface ocean forcings from two reanalyses, one from ECMWF reanalysis (ERA) or ERA15 (Gibson et al. 1997), which is available at the horizontal resolutions T106, equivalent to 1.125° in the tropics, from 1979 until 1993 and NCEP reanalysis (NRA; Kalnay et al. 1996) at the horizontal resolutions T62, equivalent to 2.5°, from the time period 1948 to 1999. These forcings have been interpolated to the model geometry.

For climatological runs, the German Ocean Model Inter-comparison Project (OMIP; Röske 2001) forcing was used. This study also made a climatological run, which was set up using the German OMIP climatology dataset as the surface forcing and was rerun for 11 years, which the first 10 years were skipped due to spin-up. The OMIP forcing was derived from the ECMWF reanalysis 15-year averages.

An independent gridded SST data from the global ice and SST dataset (GISST2; Rayner et al. 1996) version 2.3b are used in this study to validate other SST data. This dataset is compiled from SST observations from 1903–present, with a spatial resolution of 1°. To have the same period as the rainfall data, we used data from 1979 to 1993 only.

2.2 Model descriptions

Both REMO and MPI-OM are hydrostatic models working on the Arakawa-C grid for the horizontal representation. REMO requires a lateral boundary forcing at the sea surface and in each vertical layer at the boundary, while MPI-OM requires sea-surface conditions from the atmosphere.

2.2.1 The regional atmospheric model

The REgional atmosphere MOdel (REMO) is based on the 'Europa-Modell' of the German Weather service (Majewski 1991). It can be alternatively used with the physical parameterizations of the Europa-Modell or with the parameterizations of the global climate model ECHAM-4 (Roeckner et al. 1996), which were implemented at the MPI. The dynamical core of the model as well as the discretisation in space and time are based on the Europa-Modell. However, in REMO with ECHAM-4 physics not enthalpy and total water content but temperature, water vapor and liquid water are prognostic variables. In the present study, REMO with EC-

HAM-4 physics is applied. For a more detailed description of the REMO for this region, the reader is referred to Aldrian et al. (2004).

2.2.2 The ocean model (MPI-OM)

The Max-Planck-Institute Ocean Model (MPI-OM, formerly C-HOPE) is the ocean/sea ice component of the Max-Planck-Institute climate model ECHAM/MPI-OM. MPI-OM is a primitive equation model (z-level, free surface) with the Boussinesq and incompressibility assumptions, formulated on an orthogonal curvilinear Arakawa C-grid. The parameterization of net longwave radiation is based on a bulk formulae by Berliand and Berliand (1952), with the fractional cloud cover n taken as prescribed forcing. The cloudiness factor is a modified form of that proposed by Budyko (1974) and is a function of latitude only. A more detailed description of the MPI-OM is given in Marsland et al. (2003).

2.2.3 Coupling

Regional atmosphere model/MPI-OM coupling was carried out using the OASIS coupler developed by CERFACS (Terray et al. 1999; Valcke et al. 2000). The coupling procedure is similar to the one used in the MPI global climate models ECHO-G (Legutke and Voss 1999) and ECHAM-5/MPI-OM. A similar coupling procedure for a regional coupled simulation using both regional atmospheric and ocean models has also been reported (Meier et al. 2003). In this study, which differentiates from common usages, the task of the coupler is to synchronize time for coupling or data exchange only, and not to interpolate data between different grid systems. The synchronization is required because both models are running at different time steps.

The regional climate model (REMO) covers only a part of the MPI-OM area and divides the global Ocean Global Circulation Model into two subdomains: coupled and uncoupled. This peculiarity provides a requirement to run MPI-OM both in coupled and standalone modes simultaneously using additional atmospheric forcing defined in the uncoupled domain. The coupled domain is the REMO domain covering the whole archipelago (19°S–8°N, 91°E–141°E).

In the coupled domain, the ocean model receives, at a specified frequency (coupled time step), heat, freshwater and momentum fluxes which are calculated in REMO (F_{remo}), and passes back the sea-surface parameters to the atmospheric model. Outside the coupled domain, the ocean model receives, at specified frequency (forcing time step), the global, predefined atmospheric fields, which are recalculated in heat, freshwater and momentum fluxes (F_{bulk}) using bulk formulae. Note that the coupled time step and the forcing time step can be different. The fluxes, which are to be used as an ocean model forcing (F), are then the result of the following mixing scheme:

$$F = I \cdot F_{\text{remo}} + (1 - I)F_{\text{bulk}} \tag{1}$$

where I is defined as follows:

$$I = \begin{cases} 1, & \text{inside coupling/REMO region} \\ 0, & \text{outside coupling/REMO region} \end{cases} \tag{2}$$

In a normal condition, REMO-MPI-OM coupling also includes ice parameters. Since the coupled domain is located in a tropical region, the ice component is omitted. Thus the ocean only passes the SST to the atmosphere. Figure 1 illustrates the coupling processes between reanalyses, REMO and MPI-OM in coupled and uncoupled domains.

Interpolation from the atmospheric grid to the ocean's grid and vice versa is achieved in the ocean model using the so-called mosaic interpolation. Thus, the OASIS coupler sees both models on the same computational grid, i.e. the REMO grid, because it represents also the coupled domain. The interpolation scheme from MPI-OM to REMO is as follows:

$$F_{ij}^{M} = \frac{\sum_{lm} F_{lm}^{R} \cdot A_{ijlm}}{\sum_{lm} A_{ijlm}} \tag{3}$$

and from REMO to MPI-OM

$$F_{lm}^{R} = \frac{\sum_{ij} F_{ij}^{M} \cdot A_{ijlm}}{\sum_{lm} A_{ijlm}} \tag{4}$$

where F_{ij}^{M}, F_{lm}^{R} are the fields defined on MPI-OM and REMO grid, respectively. A_{ijlm} is the interpolation matrix.

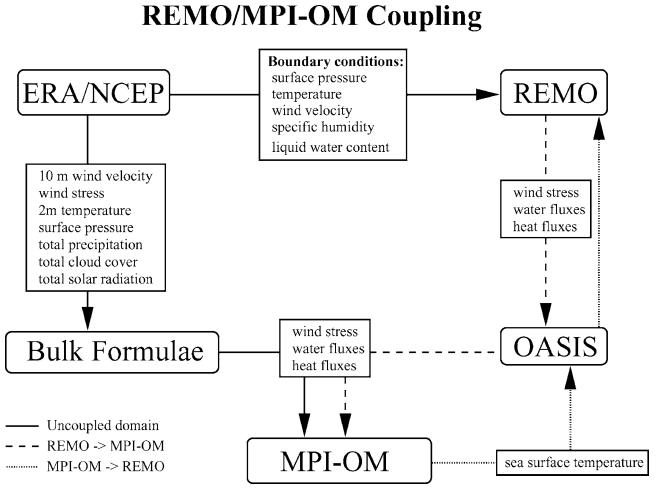

Fig. 1 A schematic view of the processes in the coupled and uncoupled domain for the ocean/atmosphere coupling of the atmospheric regional climate model REMO and the global ocean model MPI-OM, using a coupler (OASIS)

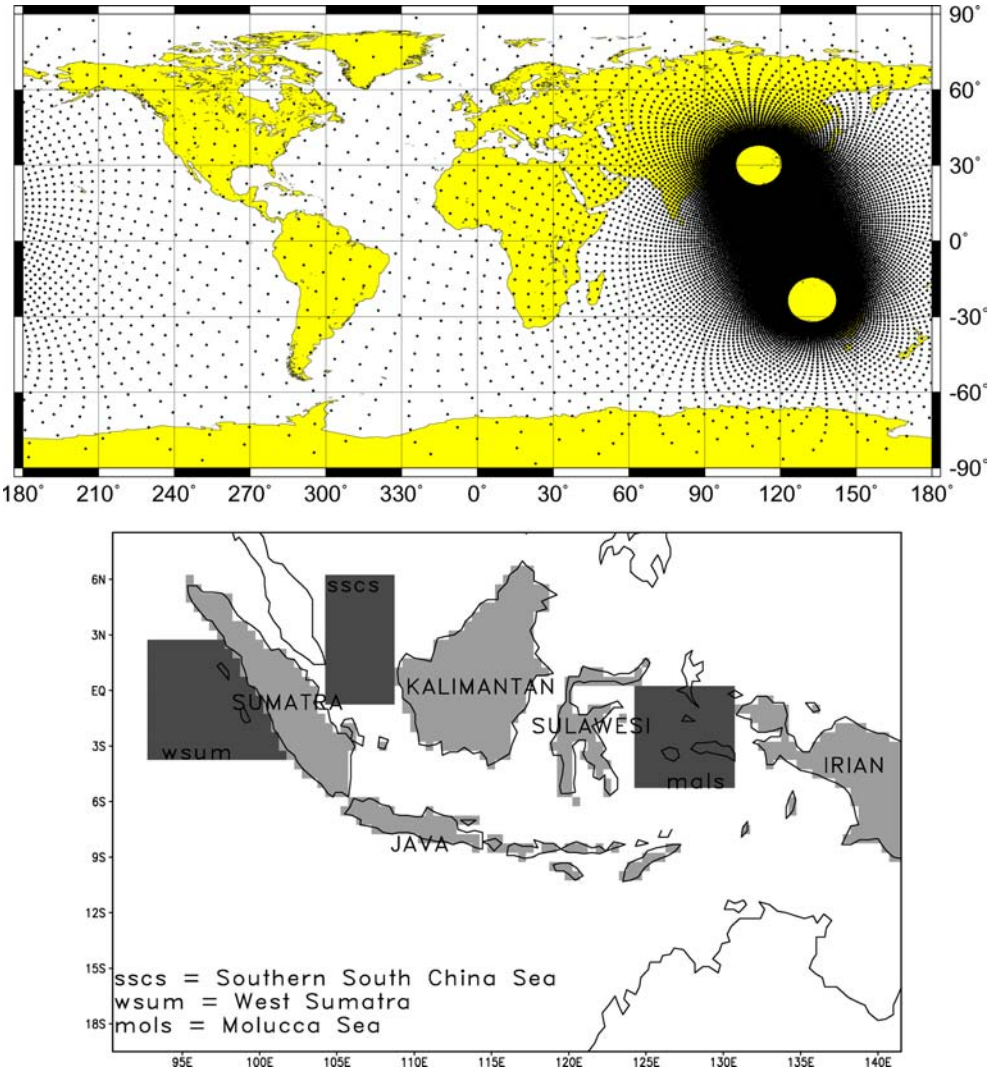

Fig. 2 The global view of the low resolution MPI-OM orthogonal curvilinear grid (*above*) and the grid system of REMO along with the five major islands and three sea areas examined in this study (*below*)

Usually, an ocean model has a much finer resolution than an atmosphere model. To take into account small-scale variability, a subscale correction of the atmospheric heat fluxes is used. As these fluxes are strongly dependent on the sea-surface temperature, this correction is assumed to be proportional to the difference between the SST calculated in MPI-OM and the same SST interpolated onto the atmospheric grid and backward. The proportionality constant, which is actually equal to d Q/d T, where Q is a heat flux and T is a surface temperature, was set according to Röske (2001) from 50 W/(m^2K) to 60 W/(m^2K).

2.3 Model setups

2.3.1 REMO setup

REMO was run in the climate mode at the resolution 0.5° or about 55 km horizontal resolution and 20 hybrid vertical levels. The REMO domain is formulated in a finite difference grid with 101 points in longitude, 55 points in latitude with a bottom left corner at 91°E/19°S or a region between 15°S–8°N and 91°E–141°E (Fig. 2). This grid system has about 21% land coverage. The model was forced with lateral boundaries from ERA15 and NRA. The lateral boundaries have a temporal resolution of 6 h and are interpolated into a 5-min time step. REMO obtains the lower boundary conditions over the sea surface from MPI-OM through the OASIS coupler at every coupling time step (6 h) and, at the same time, passes the atmospheric momentum, heat and water fluxes to the ocean model. In the uncoupled mode, REMO has its own prescribed SST from the corresponding reanalyses. The REMO used in this study allows only one type of land cover, either land, sea or ice.

A RCM has to be initialized once and supplied with lower and lateral boundary values during the whole simulation. Initialization is done for all prognostic variables in all model levels. In addition, surface temperature, soil temperatures for five soil layers down to a depth of 10 m, soil moisture, snow depth and temperature as well as the skin reservoir content

Table 1 MPI-OM ocean model descriptions

	Low-resolution	High-resolution
Meridional grid points	105	210
Zonal grid points	182	362
Layers	20	30
Mid of layer level (m)	10, 30, 50, 75, 110, 155, 215, 295, 400, 535, 700, 895, 1,125, 1,400, 1,750, 2,200, 2,750, 3,400, 4,200, 5,350	6, 17, 27, 37, 47, 57, 69, 83, 100, 123, 150, 183, 220, 265, 320, 385, 460, 550, 660, 795, 970, 1,220, 1,570, 1,995, 2,470, 2,970, 3,470, 4,020, 4,670, 5,520
North Pole	112°E 29°N	
South Pole	132°E 22°S	
Time step	3,200 s	1,440 s
Input/Output	6 hourly/monthly	
Cell size (Banda Sea)	0.391° (40 km)	0.202° (20 km)
Max. cell size (west equatorial Atlantic)	8.20° (800 km)	3.88° (370 km)
Input forcing (OMIP climatology, cNCEP/NCAR and ERA 15 reanalyses)	2 m air temperature short wave radiation forcing precipitation rate cloud cover dew point temperature zonal (u) momentum surface flux meridional (v) momentum surface flux 10 m wind velocity	

(water stored by the skin of the vegetation) must be supplied.

2.3.2 *MPI-OM setup*

The MPI-OM uses a bipolar orthogonal spherical coordinate system, which allows irregular positions of the poles. This study uses a special conformal grid where the North Pole is located in China (112°E–29°N) and the South Pole in Australia (132°E–22°S). This pole placement offers two major advantages over regular latitude–longitude grids. Firstly, the placement of the poles over land removes the numerical singularity associated with the convergence of meridians at the geographical north pole. Secondly, the choice of nondiametric poles allows for the construction of regionally high resolution models that maintain a global domain and thus avoid the problems associated with either open or closed boundaries. However, it should be noted that this approach has the disadvantage of globally constraining the model time step to one small enough to be appropriate for the highest resolution region. This limitation will be analyzed with different resolutions in the present study. Figure 2 illustrates this conformal grid with a global view. The minimum cell size is located near the poles. In Table 1, selected information on the model setup are presented. The higher resolution grid is characterized by a double horizontal resolution and 30 vertical levels (as opposed to 20 levels in the coarse resolution) with increasing level thickness from surface to bottom. The horizontal resolution gradually varies between a minimum of about 15 km near the poles and a maximum of 370 km (high-resolution mode) in the western edge of equatorial Atlantic. MPI-OM is a hydrostatic ocean model, which uses z-coordinates for vertical discretisation.

The MPI-OM is started from the stand-alone mode and it is initialized with climatological temperature and salinity data (Levitus et al. 1998). It is then integrated for

Table 2 Fifteen-year correlations between rainfall simulations and rain gauge observations for reanalyses, uncoupled REMO and two coupled REMO simulations over the five major islands

	Java	Kalimantan	Sumatra	Sulawesi	Irian
NCEP					
Global reanalysis	0.708 (39.2)	0.783 (4.2)	0.666 (18.3)	0.693 (8.5)	0.507 (10.9)
Uncoupled REMO	0.722	0.702	0.716	0.609	0.403
Coupled low ocean	0.777 (11.8)	0.763 (10.4)	0.740 (31.6)	0.626 (39.6)	0.437 (34.6)
Coupled high ocean	0.787 (7.5)	0.766 (9.1)	0.749 (25.5)	0.600 (45.1)	0.445 (31.6)
ERA					
Global reanalysis	0.822 (30.9)	0.803 (49.3)	0.779 (15.3)	0.472 (0.3)	0.442 (31.2)
Uncoupled REMO	0.804	0.800	0.732	0.669	0.483
Coupled low ocean	0.826 (26.4)	0.786 (32.6)	0.721 (41.4)	0.673 (47.0)	0.490 (46.3)
Coupled high ocean	0.823 (29.3)	0.776 (24.4)	0.713 (35.7)	0.650 (37.8)	0.509 (37.1)

All correlation values have 0.01% significant levels on two sides of all data. Numbers in brackets are significances of differences between correlations of the uncoupled REMO with others. All values are in percent and significant for one side

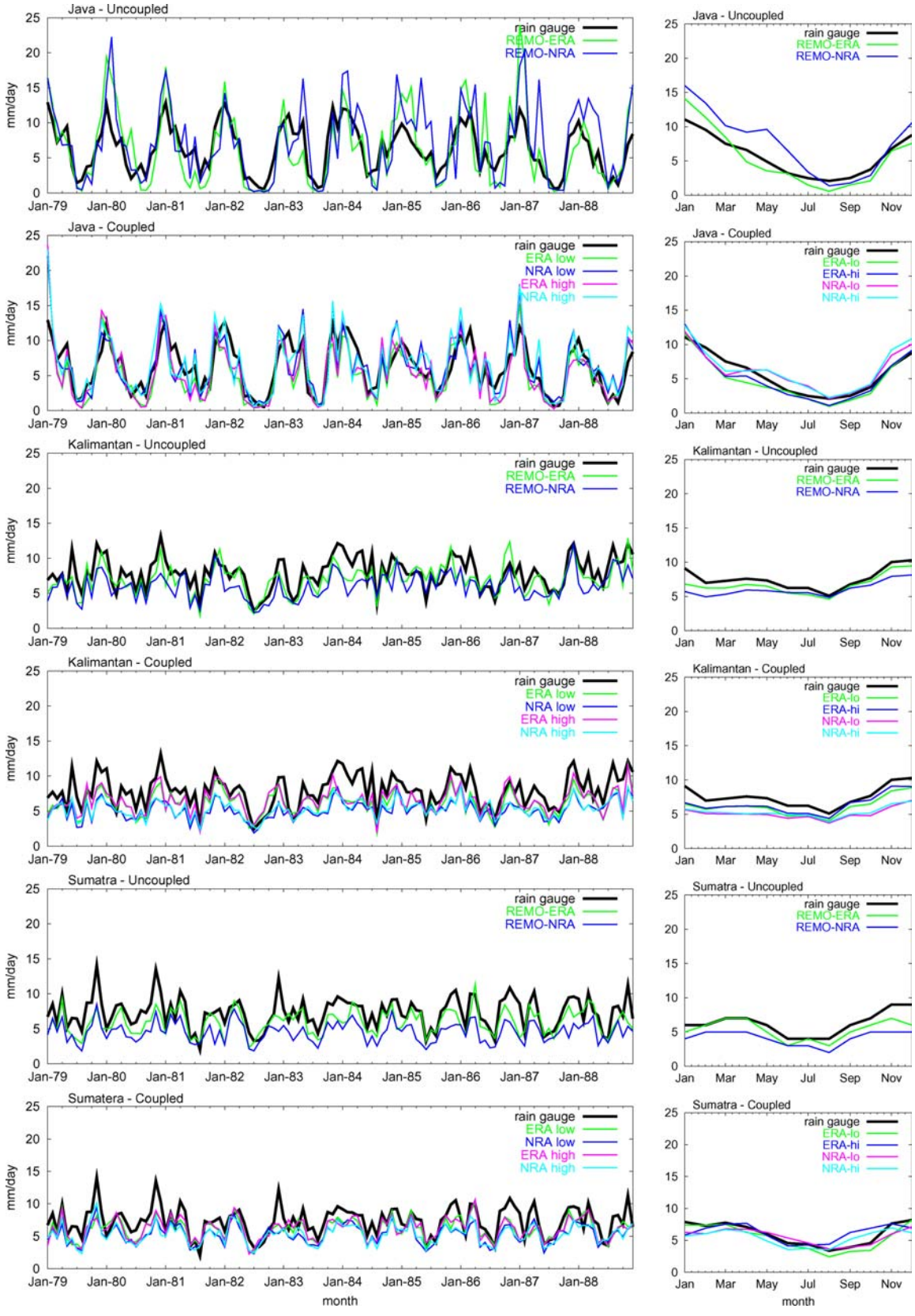

Fig. 3 Weighted area averages of the variability of simulated (uncoupled and coupled) and observed rainfall for the five major islands (*left*) and their corresponding monthly means (*right*). For clarity reason, only the first 10 year variabilities are shown

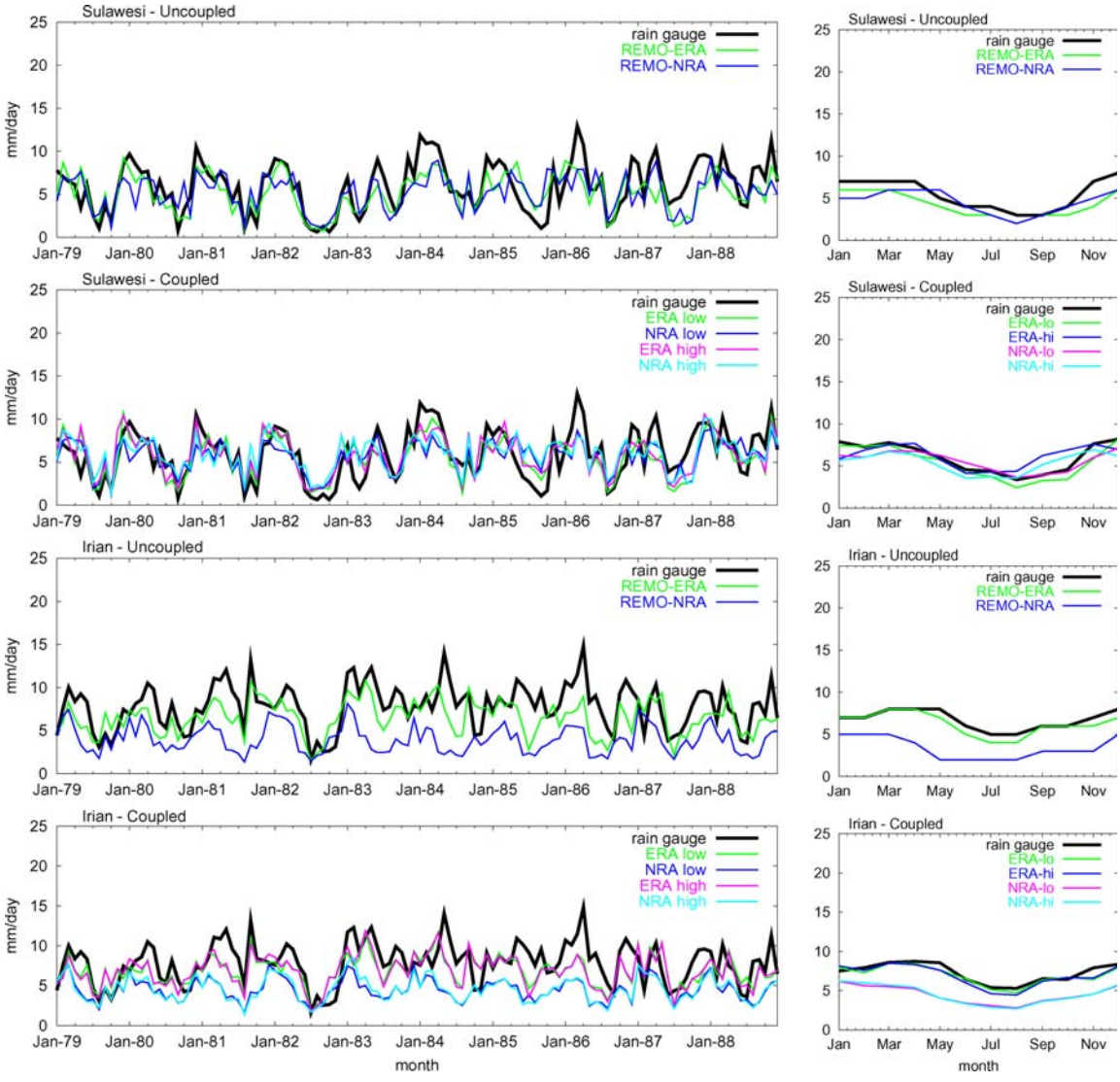

Fig. 3 (Contd.)

31 years from 1948 to 1978 using 6 h NCEP reanalysis data as forcing. This period of this integration is used as spin-up.

2.3.3 Coupling experiments

In the coupled mode, the model is started from the state obtained by the stand-alone runs after the spin-up. The initial date is 01.01.1979 and it is integrated until 31.12.1999. Atmospheric forcing, calculated from NCEP reanalysis data is applied every 6 h. At that same time, the ocean model gets atmospheric fluxes calculated in REMO and passes sea-surface temperature to REMO. The coupled REMO/MPI-OM experiments covered the period from 1979 to 1993 for both reanalyses and additionally up to 1999 for NCEP in order to account for the Indonesian Throughflow study (see Sect. 4.1). The Indonesian throughflow study cannot be performed with ERA data due to limited reanalysis data up to 1993. One simulation was performed for each reanalysis and at two resolutions of MPI-OM. In total, for two reanalyses and two resolutions, there are 66 years of integration. During the whole experiment, instead of the salinity relaxation procedure, only the constant freshwater flux correction was used. No heat and momentum flux corrections were applied during the entire coupling experiments.

The model output consists of two parts: the atmospheric and oceanic. REMO output is based on the REMO's rotated Arakawa C-grid with 20 vertical hybrid levels and is stored with 6-h time interval. The ocean dataset, omitting the sea-ice parameter output, is written on the MPI-OM orthogonal curvilinear Arakawa C-grid with 20 (low-resolution) and 30 (high-resolution) vertical levels as monthly mean values.

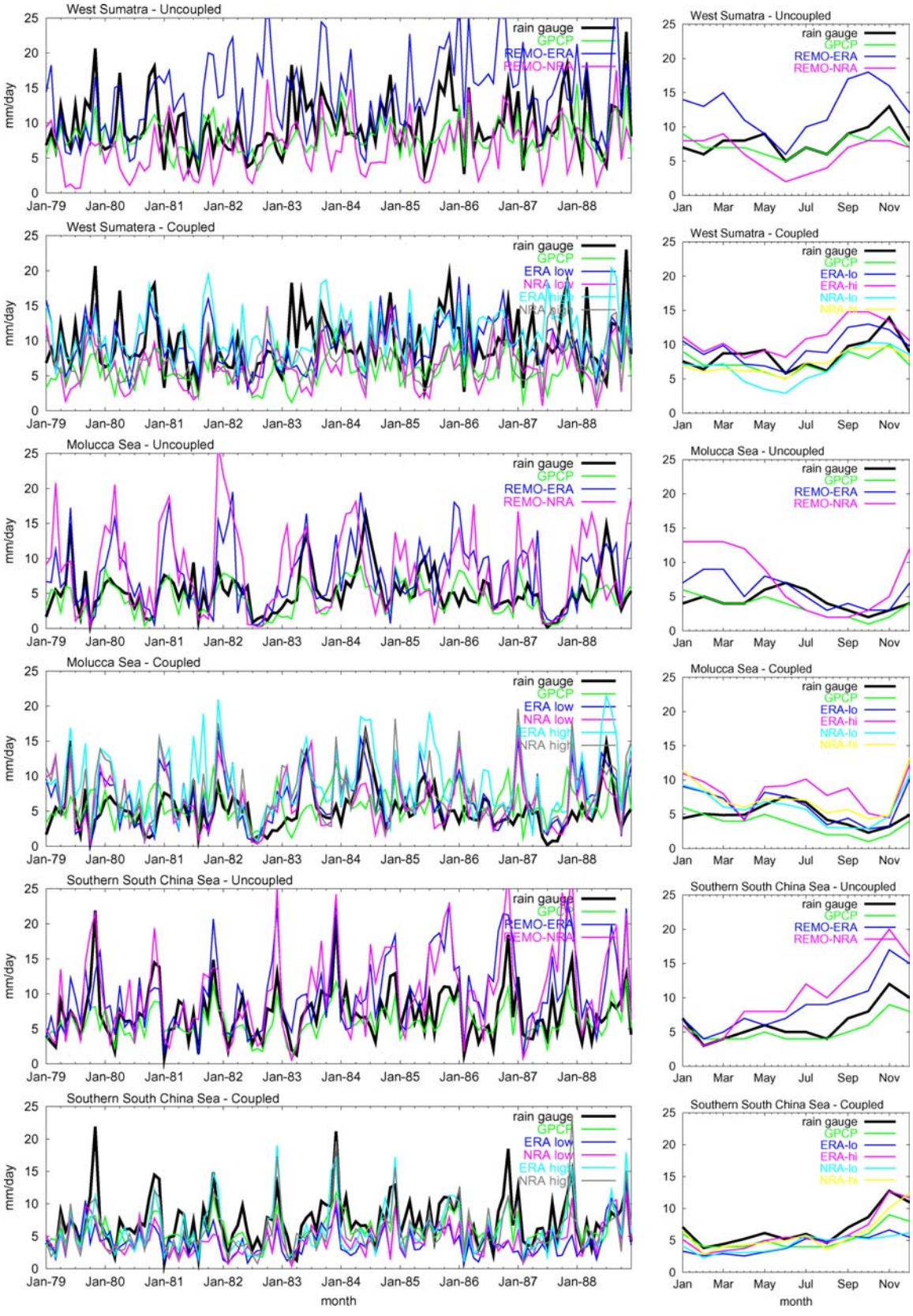

Fig. 4 Weighted area averages of the variability of simulated (uncoupled and coupled) and observed rainfall for the three sea areas (*left*) and their corresponding monthly means (*right*). For clarity reason, only the first 10 year variabilities are shown

Table 3 Fifteen-year correlations between global reanalyses, uncoupled REMO and two coupled REMO and observations over the three sea areas

	WSUM	MALS	SSCS
NCEP			
Global reanalysis	0.133* (16.9)	0.534* (0.5)	0.675* (47.7)
Uncoupled	0.232***	0.312**	0.679*
Coupled low ocean	0.317** (19.3)	0.489* (2.4)	0.535* (1.6)
Coupled high ocean	0.311** (20.9)	0.519* (0.9)	0.726* (18.8)
ERA			
Global reanalysis	0.418** (43.3)	0.259** (0.01)	0.771* (7.2)
Uncoupled	0.433*	0.581*	0.700*
Coupled low ocean	0.431* (49.2)	0.650* (14.8)	0.579* (2.6)
Coupled high ocean	0.437* (48.1)	0.696* (3.3)	0.746* (18.1)

One, two and three asterisks indicate correlation at the 0.01, 5 and 10% significance levels on two sides of all data, respectively. Numbers in brackets are significances of differences between correlations of the uncoupled REMO with others. All values are in percent and significant for one side

3 Implications for the atmosphere

This section presents rainfall variability from the coupled model integrations, the uncoupled REMO model described in Aldrian et al. (2004) and their comparisons to the observed data. The stand-alone model results will not be covered in detail here. We will look at the rainfall variabilities for the five major islands and three sea regions as illustrated in Fig. 2.

3.1 The five major islands

Figure 3 shows variabilities of the monthly mean rainfall from the coupled REMO-MPI-OM simulations from two reanalyses with two different ocean resolutions and their uncoupled REMO simulation counterparts for the five major islands. There are no notable differences between simulations with different ocean resolutions except for Sumatra and Sulawesi or, in other words, the lateral boundary and reanalyses play stronger role here. From that figure, Java seems to have the best performance after coupling, where REMO does not produce under- or overestimations as large as on the other islands. Within all other islands REMO simulations tend to underestimate, and the largest underestimation occurs in Kalimantan and in Irian with the NRA forcing. In the coupled simulations, REMO performances improve over Java, Sumatra and Sulawesi quite well. Strong improvements of those islands are obvious from the annual average figures. Between the two reanalyses, ERA forcing leads to better performances than NCEP (except for Sulawesi). The latter fact is obvious from the 15-year averaged, monthly mean figures.

The summary of the correlations between original reanalyses or REMO simulations and rainfall observation is given in Table 2. We then use the Fisher's z-transformation (Press et al. 1996) to calculate the approximately normally distributed correlation values as given below

$$z = \frac{1}{2}\ln\left(\frac{1+r}{1-r}\right) \tag{5}$$

Using the above z values, the significance of a difference between two measured correlation coefficients on two sides is defined by

$$erfc\left(\frac{|z_1 - z_2|}{\sqrt{2}\sqrt{1/(N_1-3)} + \sqrt{1/(N_2-3)}}\right) \tag{6}$$

All significant differences between uncoupled REMO simulations and others are presented in Table 2 for values in the brackets. For the case of the NCEP analysis in Java, there is about 19% improvement from the original reanalysis to the coupled simulation and about 9% in Sumatra and their corresponding significant differences. For other islands, REMO simulations could not produce correlation as high as the original reanalysis. However, among the REMO simulations, there is a small improvement by coupled REMO with high-resolution ocean model. For the case of ERA reanalysis, improvements occur in Java, Irian and the largest in Sulawesi of about 18%. Among REMO simulations coupling does not always produce a better result. In fact, the improvement by coupling in comparison to the uncoupled model is in general, rather small. For both reanalyses, the best performance is in Java, which has a homogenous climate region (the monsoonal region), while other islands experience a combination between different monsoonal systems (Aldrian et al. 2003). Kalimantan has the second best performance followed by Sumatra and Sulawesi. Irian has the lowest performance in both reanalyses, which is mainly due to boundary zone problem. This island is located in the REMO boundary zone, where the coarse resolution lateral boundary has still some influence. In general, Table 2 shows that

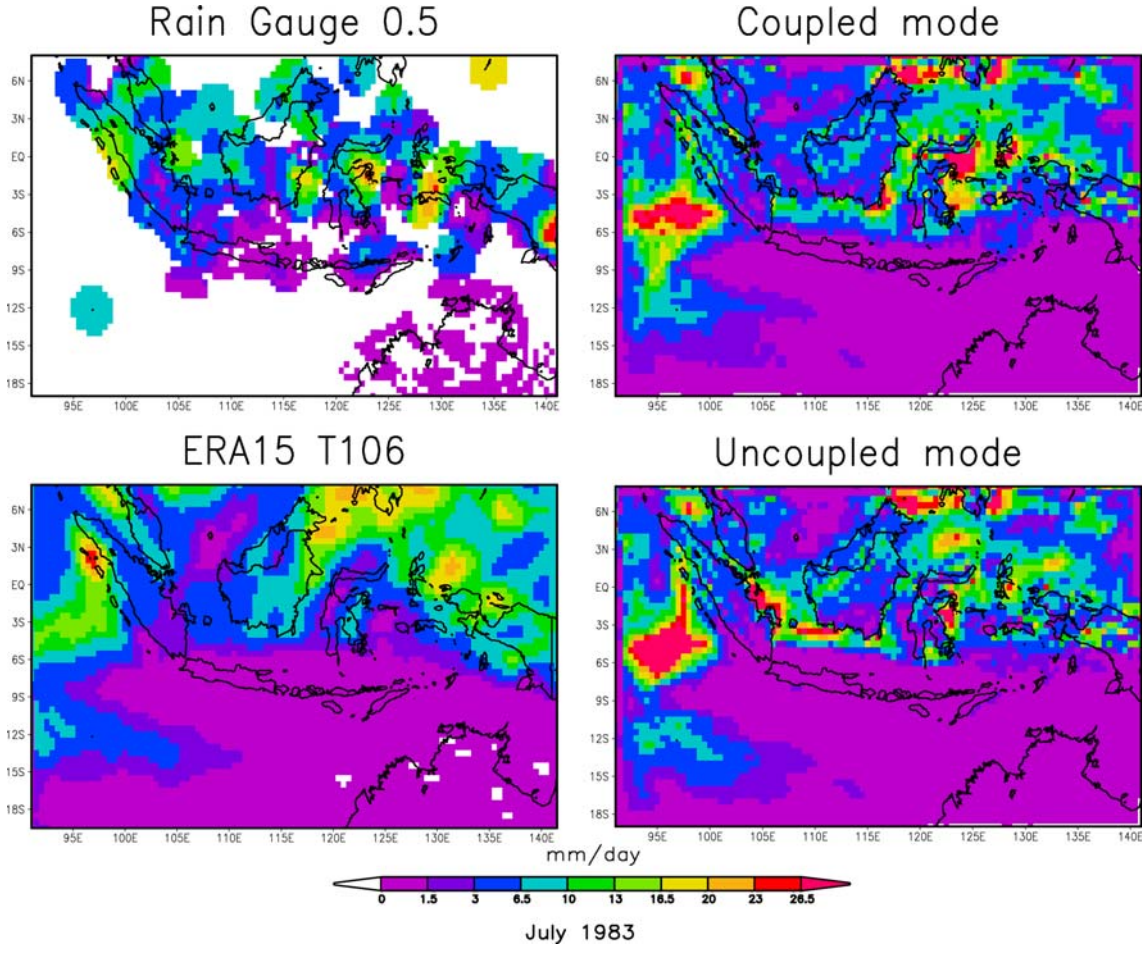

Fig. 5 Comparison of three rainfall simulations and observation, from land-based rain gauges for July 1983. The coupled mode stands for REMO/MPI-OM with high resolution of the ocean model MPI-OM

the quality of the reanalysis largely determines the quality of the REMO result.

3.2 The three sea regions

The variabilities of REMO simulations for the three sea areas are given in Fig. 4. The three sea regions are West Sumatra (WSUM), the Molucca Sea (MOLS) and the southern part of the South China Sea (SSCS), which represents the monsoonal, anti-monsoonal and semi-monsoonal region, respectively, following the three major climate regions of Indonesia according to Aldrian and Susanto (2003). In comparison to the uncoupled simulation results, there is less overestimation in all three regions and the improvements are obvious from their annual mean figures than in the uncoupled simulations. The much greater coherence among the coupled simulations should be noted. In uncoupled simulation, REMO-ERA gives much too high estimations over the sea, which turns out to be the major problem of REMO simulations in this region. Like in the case of simulations over land, coherence between similar reanalysis for two different ocean model resolutions is high (especially with

Table 4 Major Seas and straits

No.	Area or section	Start position	End position	Remarks
1.	South China Sea	112.0E 8.0N	106.1E 1.8N	
2.	Karimata Strait	106.1E 1.8N	109.2E 5.0S	Between Sumatra and Kalimantan
3.	Java Sea	109.2E 5.0S	116.1E 5.8S	Ocean depth 50m
4.	Makassar Strait	116.1E 5.8S	120.2E 4.0N	Between Kalimantan and Sulawesi
5.	Sulawesi Sea	120.2E 4.0N	131.0E 2.9N	Between Sulawesi and Mindanao
6.	Halmahera Strait	131.0E 2.9N	129.1E 2.1S	Between Halmahera and Irian
7.	Seram Strait	129.1E 2.1S	131.5E 4.7S	Between Seram and Irian
8.	Banda Sea, Timor Sea	131.5E 4.7S	124.0E 14.S	Between Australia and Timor

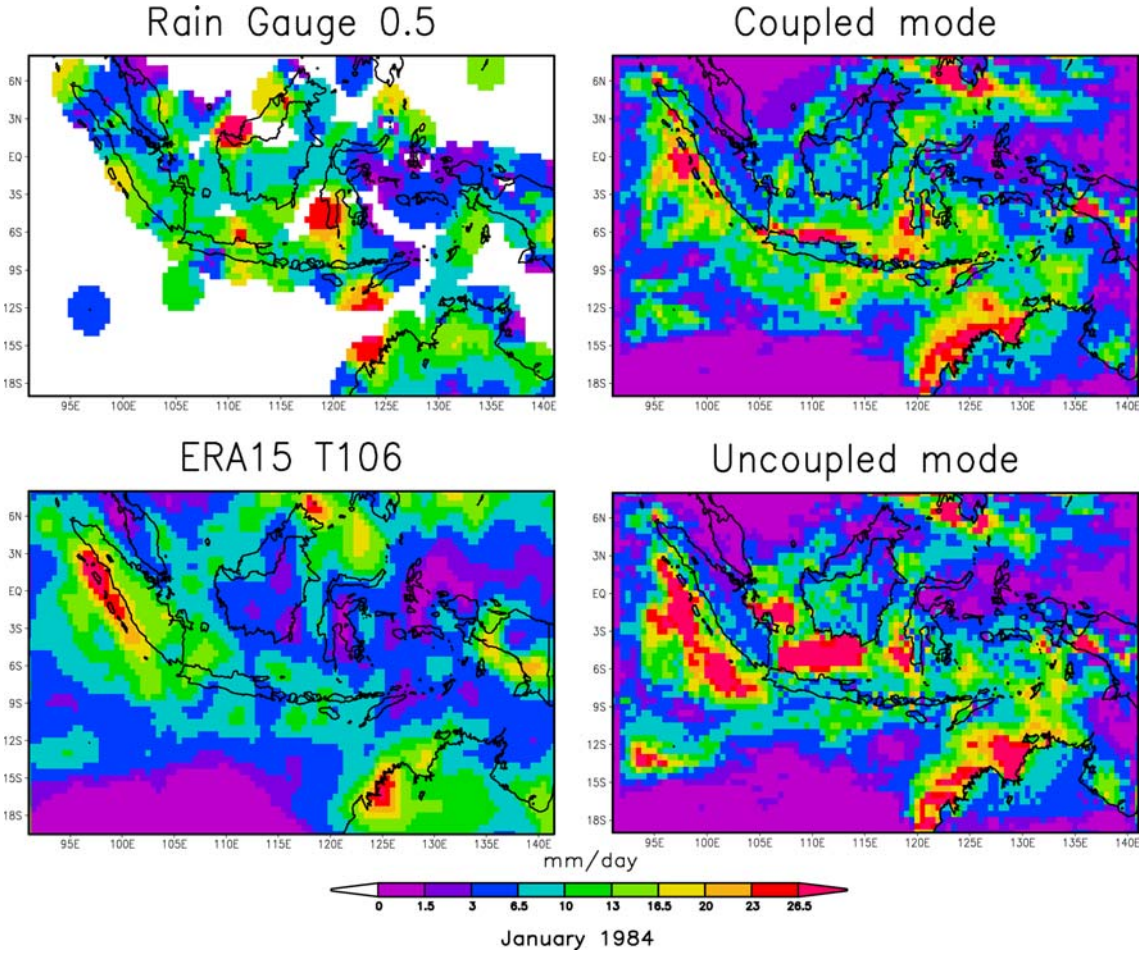

Fig. 6 As Fig. 5, but for January of 1984 (a non ENSO year)

NRA). In other words, the type of reanalysis plays a greater role than the resolution. Over the Molucca Sea, the coherence among all REMO simulations is high, except for some cases with the ERA forcing coupled with the high-resolution ocean model and for REMO-NRA over Molucca Sea. In the Molucca Sea, most REMO simulations overestimate rainfall, while, on the other hand, in the South China Sea, most REMO simulations underestimate. Regardless of these small drawbacks, the too large overestimation over the three sea regions in the uncoupled REMO (Fig. 3) has been reduced considerably for the coupled REMO. The simulation in the South China Sea seems to be the best among the three sea regions (see Table 3), followed by the Molucca Sea. In comparison to the analyses of five major islands, coupling processes improve REMO performances over the sea regions better than those over the major islands.

The summary of correlation between reanalysis or model simulations and observation over the three sea regions is given in Table 3. In two of three regions of each reanalysis, there are some improvements in coupled REMO simulations and their corresponding significant differences, especially over the Molucca Sea from the original ERA reanalysis for about 46%. Among NCEP simulations, most have improved from uncoupled to coupled model except for West Sumatra. Among ERA simulations, WSUM and MOLS have improved. In fact, this region has the lowest correlation in comparison to other regions in different reanalyses. Low correlation in West Sumatra is also due to low quality of observation in the area. The observation data comprises only inland station data while the ocean data have been interpolated.

3.3 Precipitation reduction over the sea

In Aldrian et al. (2004) or the uncoupled simulation, the overestimation of rainfall over the sea is one of the difficult problems faced by REMO. Some sensitivity studies have been performed in order to understand the problem, but none has passed the criteria of lowering the precipitation amount over the sea, while maintaining the accumulated inland precipitation amount. The inland precipitation by REMO has performed well in comparison to the observation. One promising solution from these sensitivity studies is the reduction of SST by 1°C. The result was a high reduction of precipitation over sea

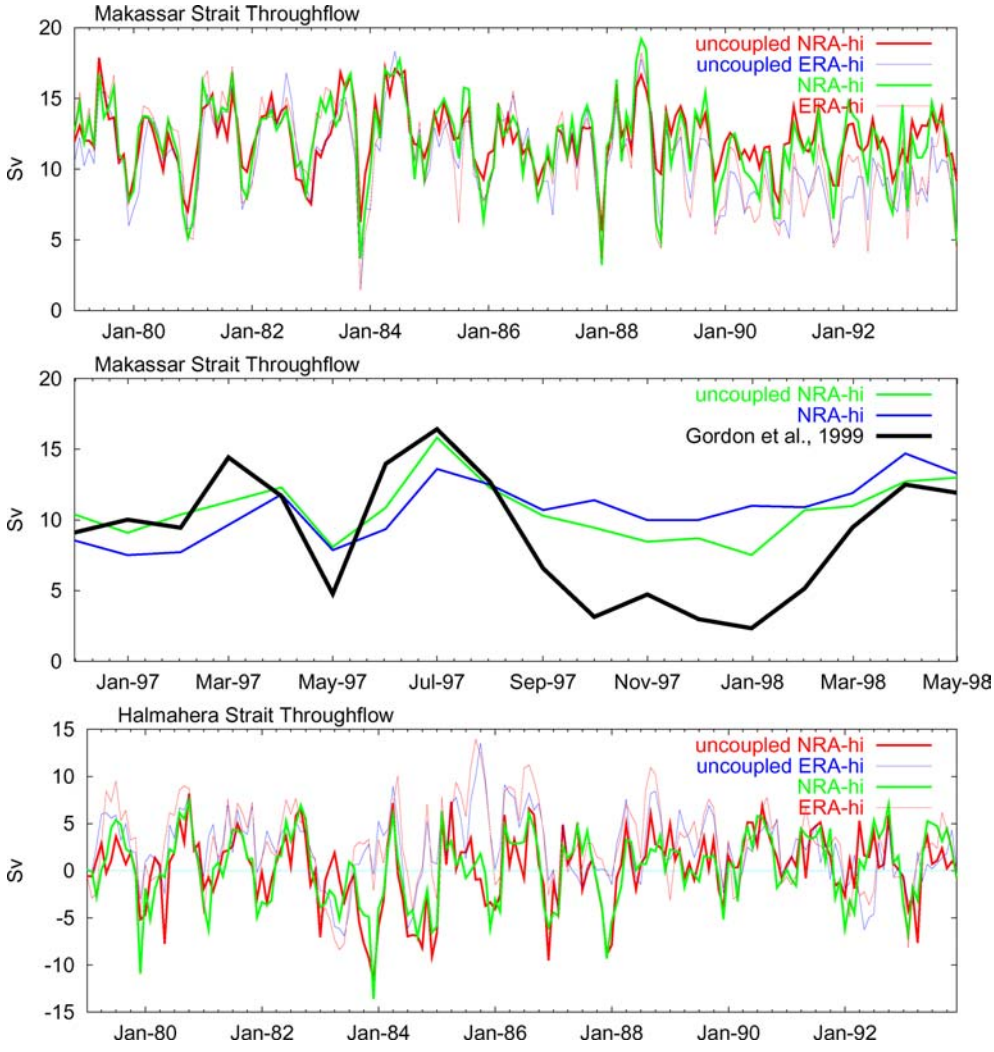

Fig. 7 Makassar and Halmahera Straits throughflow as simulated by the coupled REMO-MPI-OM and a comparison to observations for Makassar Strait

and a small reduction over land. However, with the current coupled model, SST is no longer prescribed but derived from the ocean model calculations.

Figures 4 and 5 illustrate two examples of the coupling effect over the sea by REMO in comparison to the original reanalysis and to the observations. The examples are taken from a non-ENSO year for boreal summer (Fig. 4) and winter (Fig. 5). The two figures indicate the overestimation of precipitation over the seas by the uncoupled REMO simulations. The overestimations have been reduced in the coupled mode. The boreal winter case illustrates a better example with a strong reduction of overestimations from the uncoupled to the coupled mode. Although correlations between coupled and uncoupled are similar, there is an improvement because of a smaller overestimation of rainfall over the sea.

4 Implications for the ocean

This section presents results from coupled model integrations and their comparisons to the uncoupled MPI-OM model as described in Table 1. Thus, the standalone model result will not be described in detail here. We will look at the variabilities of the Indonesian throughflow, SST and thermohaline circulations and focus over eight major sections from a continuous polygon of Indonesian seas. The polygon sections will be used in each vertical profile analysis, where the inset figure in each contour map represents the major sections of Table 4 starting from Sect. 1 (on the left end of each contour map) in the South China Sea.

4.1 Variability of throughflow

The coupled model simulations of the variability of two major throughflows (the Makassar and the Halmahera Straits) are given in Fig. 6. There is a slight contrast between the results of uncoupled and coupled models; however, within the Halmahera Strait and in some years, differences are eminent. The coupled mode throughflow in the Halmahera Strait, in comparison to the uncoupled model, shows more variability and more southward transport. In comparison to the low-resolution coupled

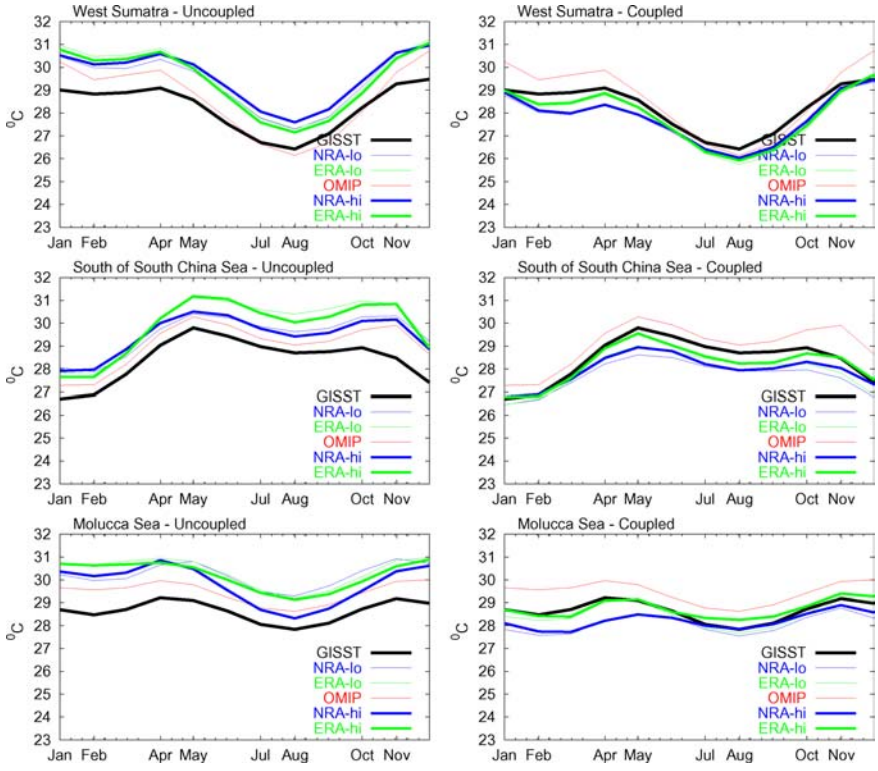

Fig. 8 Sea surface temperature variability from REMO simulations and comparison to observations as well as simulations within OMIP for the three sea areas

model (not shown), the high-resolution model produces more vigorous flow and more high frequency variability in both straits. Due to poor observations both in time and space, only few studies have addressed the oceanic variation in this region. Here, we use the in-situ observation from November 1996 to July 1998 of the water transport (Gordon et al. 1999) from the Arlindo project. In comparison to the observed Makassar Strait throughflow (Gordon et al. 1999) in the middle panel, the coupling has damped the variability from September 1997 until February 1998 more than the high-resolution uncoupled model. There is more southward transport over that period. This result is unexpected, because in the long simulation of the throughflow in the top panel of Fig. 6, the coupled model calculates stronger variability. Thus, the uncoupled mode produces a better simulation than the coupled one.

4.2 SST Variability

The SST variability of the three sea regions from the coupled simulation as shown in Fig. 7 is closer to observation (GISST) than that of the uncoupled ocean model. The uncoupled ocean model had an almost 2°C warm bias all over the places. The OMIP forcing simulation has the least biases among the uncoupled model. On the other hand, all results after coupling, especially with ERA forcing, are better than the climatological run with the OMIP forcing at the low-resolution uncoupled model. In all three sea regions, the ERA high-resolution coupled model produce almost aligned annual variability to observation. In most cases, there is a close agreement between coupled model results with the same forcing at different resolutions. Between two different forcings, ERA forced simulations produce better SSTs. The significant improvement by the coupled model shows the solution of the warmer biases in the uncoupled model due to bulk formulae. However, the uncoupled model follows the SST variability quite well but not in the correct magnitude. Inside the limited coupled region, the sea-surface atmospheric fluxes are calculated using the dynamic input from the REMO model instead of using the bulk formulae. Besides, the atmospheric regional model works at a higher resolution than the original reanalysis, thus providing better atmospheric fluxes to the ocean.

4.3 Mean thermohaline condition

In order to understand the implication of coupling to sea-surface flux exchange better, we will analyze vertical profiles of the mean thermohaline differences. Figure 8 shows the mean difference of the vertical temperature profile in the upper ocean between the coupled and the uncoupled model. Most differences are confined to the upper 200 m. In comparison to the uncoupled mode, there is a 2°C lower surface temperature all over the place and 1°C higher temperature at around 100 m depth in January in the eastern seas and in July in the South China Sea and the Karimata Strait. The lower surface temperature is associated with

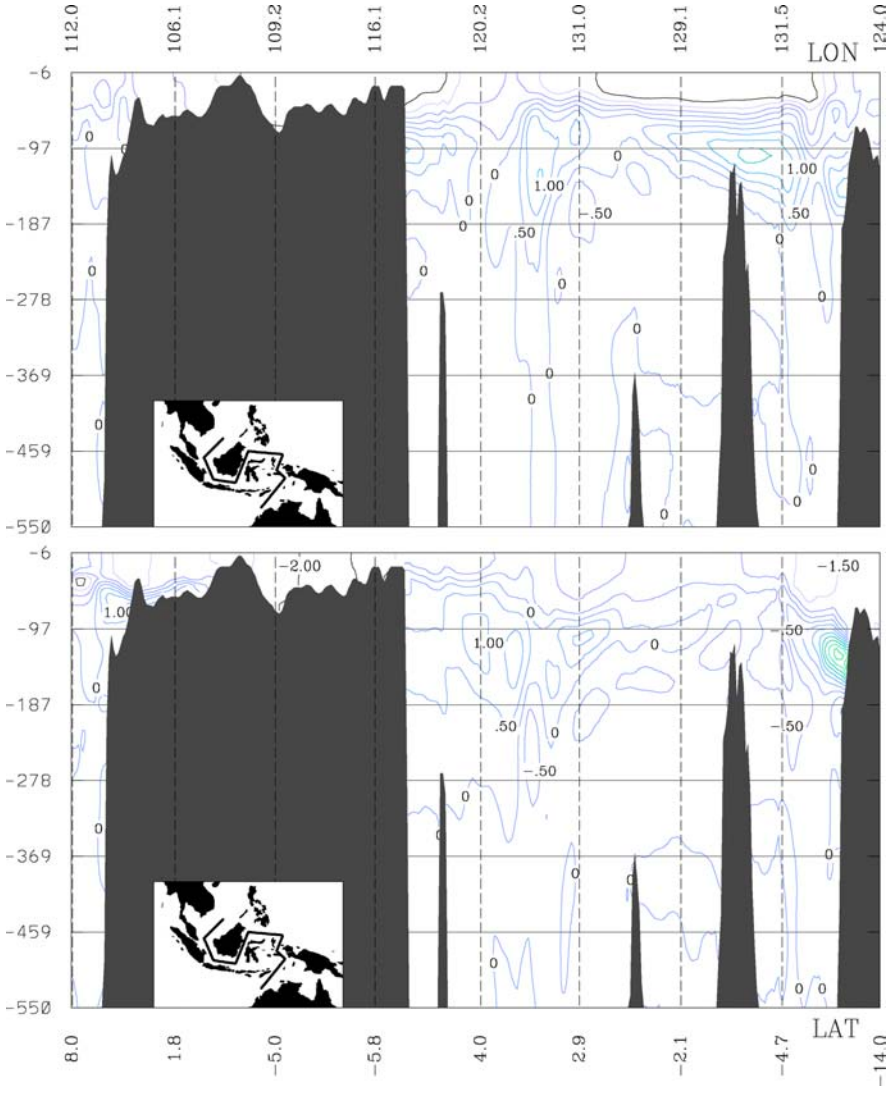

Fig. 9 Differences of the mean vertical temperature profile in January (*above*) and July (*bottom*) for the years 1979–1993 between coupled and uncoupled mode of MPI-OM-NRA in high resolution. Contour interval is 0.5°C. The inset shows the geographic location of the section following Table 4. Labels show depth in meter (*ordinate*), latitude (*bottom abscissa*) and longitude (*top abscissa*)

the warm bias probably originating from the bulk formulae in the uncoupled model. In the southern edge of the Banda Sea at around 150 m, there is a 4°C lower temperature in July and 1°C lower temperature in January. In January in Seram Strait, there is 1.5°C higher temperature.

The mean salinity difference between the coupled and uncoupled model is given in Fig. 10. Most differences take place in the upper 100 m and rather in January than in July. January is the peak of the wet season, when most precipitation takes place, thus fresher seawater (indicating by minus sign in Fig. 9) is expected by high amount of surface water input. Large differences occur in the shallow water regions of the Karimata Strait and the Java Sea. However, the absolute difference between coupled and uncoupled run is small for both months with a maximum difference of 0.25 psu. In January, there is a fresher (less saline) water layer near 70 m depth in Sulawesi Sea and the Halmahera Strait. In January the water is fresher in the coupled model for most regions of the upper 100 m layer.

5 Discussions and concluding remarks

Simulations of the Indonesian climate using a special coupled model setup with a Regional Climate Model, REMO, and an Ocean Global Circulation Model (MPI-OM) with boundary forcings from two reanalyses have been performed. We analyzed the results with the comparison to the uncoupled ocean and atmosphere models. The analysis focuses on the rainfall variability for the atmospheric part and SST and ocean circulation for the oceanic part. With our special model setup and without flux correction, the coupled model is able to produce stable and realistic rainfall variabilities. In fact, in most cases, performances of the coupled model simulations are better than the uncoupled ones.

Our study was motivated by the unsatisfactory result of some rainfall patterns in the uncoupled climate model for this region. The uncoupled atmospheric model had a major drawback in overestimated rainfall over the sea

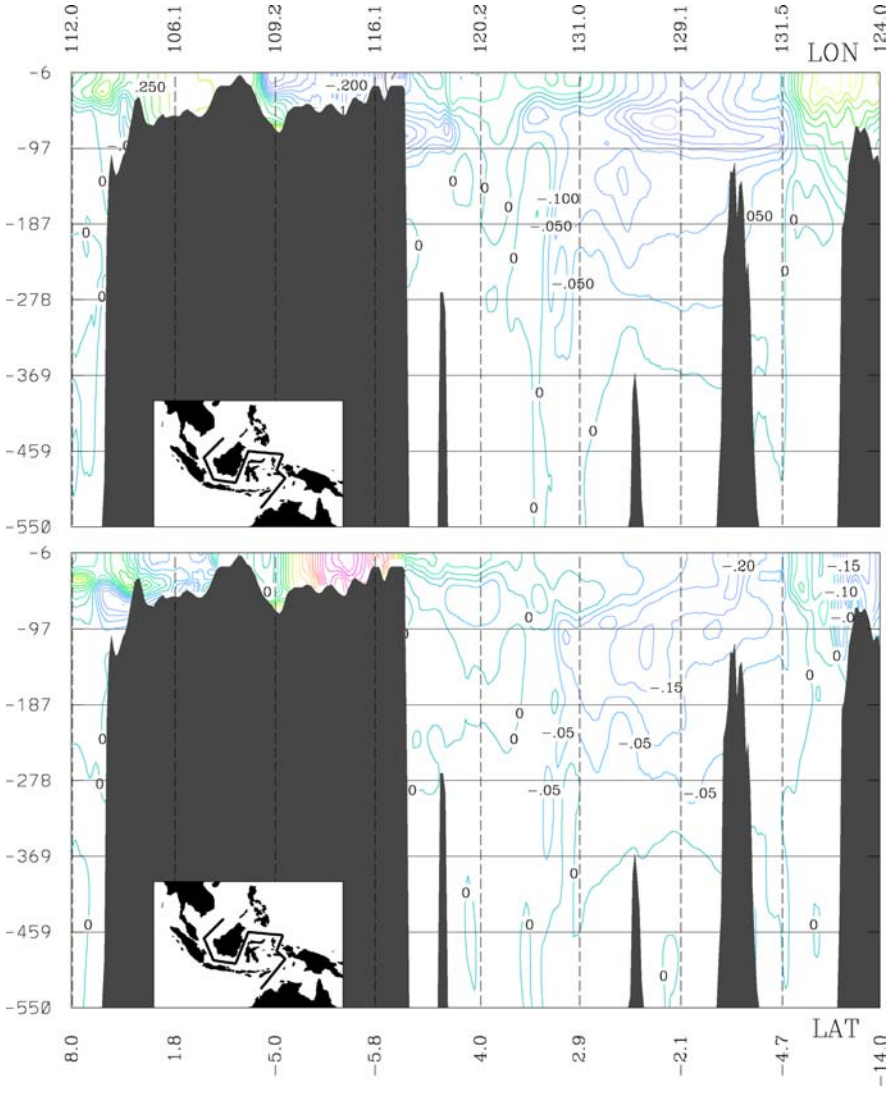

Fig. 10 As Fig. 9, but for salinity. Contour interval is 0.05 psu

(Aldrian et al. 2004). The uncoupled ocean model, on the other hand, had a problem with the bulk formulae for heat fluxes, which consequently lead to a warm SST bias over the region. The coupled climate model has successfully reduced these problems. With a coupled model, we give more degree of freedom to both models. In the uncoupled ocean model, the forcing is prescribed from the atmospheric reanalyses and recalculated to provide surface water and heat fluxes for the model using an empirical bulk formulae. Such an approach suffers large effect in this archipelago, since the bulk formulae are applied globally and may not be suitable for local and regional use. This deficiency is reduced in a coupled model, because the RCM improves the coarse resolution of the reanalyses and thus provides a higher resolution atmosphere in the coupled region. Moreover in the coupled domain, the ocean model does not receive flux calculations from the bulk formulae, but directly from the atmospheric model.

The ocean in the coupled mode gives feedbacks to REMO with a higher resolution SST than the original SST from the global reanalysis. In the uncoupled mode, the SST is obtained from an interpolated coarser resolution reanalysis and this SST is a static supply, which does not respond to any dynamical processes in the atmosphere. In the coupled mode, the dynamics in the atmosphere changes the ocean, which consequently changes the SST. Besides, the rainfall is a stochastic process, where the dynamics of some previous feedbacks is important. Thus the accumulated errors by few consecutive supplies of SSTs provide wrong feedbacks to the precipitation processes. This stochastic error will be reduced by better dynamics from the ocean feedback. Hence, the two figures illustrate two step improvements by REMO from the original reanalyses. Firstly, there is an improvement by better orography, which contributes to better atmospheric dynamics in a higher REMO resolution. However, the improvement is confined to the quality of the lateral boundary condition from the reanalysis (Table 2 and 3). Secondly, a better dynamic in a higher resolution SST also determines the quality of

the simulation result. Although correlations between coupled and uncoupled are similar in coupled and uncoupled REMO, there is an improvement in the absolute amount of overestimations over the sea (Fig. 4 and 5).

There are only small differences in rainfall variability for two different ocean resolutions and the difference is mainly due to the quality of the reanalysis. However, in the ocean, different resolutions play a greater role than the atmospheric forcing type. The results also show that the improvement for inland rainfall is very small, but for rainfall over the ocean, it is remarkable. Much of the improvements over the sea can be attributed to the reduction of rainfall overestimation. Thus, large improvement in the atmosphere is due to an introduction of a dynamic change of SST from the uncoupled to the coupled model.

The analyses of the ocean model simulations show the importance of a correct bulk formulae. In the coupled mode, the model simulates the SST variability well. One possible parameter that plays a significant role in the bulk formulae is the cloud cover, which is badly represented in the reanalyses and the global climate model (Jakob 2000). Although the coupling occurs only for a limited domain, the SST variability and ocean circulation has changed drastically compared to the uncoupled mode. With regard to the stratification, the coupling changes the temperature and salinity profiles in the upper 200 m and 100 m, respectively. Thus, changes in ocean dynamics in the upper 200 m are very important in regulating the local SST and, eventually, the precipitation pattern.

In summary, the coupling has positive implications for the atmosphere and the ocean. There is less overestimation of rainfall over the sea and a more realistic representation of SST. However, coupling reduces the variability of the throughflow. Both reductions of the rainfall over the sea and the variability of the throughflow show that the coupling damps the atmospheric and ocean circulation. In comparison to previous results from the uncoupled climate model, the rainfall simulation over this region has been simulated best with the high-resolution coupled model. This study uses only one spatial resolution in the atmosphere model and two ocean resolutions. It is desirable to extend the work with different atmospheric resolution to investigate the role of different resolution on the model simulation. The present simulations and analyses are confined to the ERA15 period. It is also desirable to extend the work with the new ERA40 (Simmons and Gibson 2000) and the whole NRA dataset.

Acknowledgements The first author is very grateful for the DAAD scholarship A/99/09410. We thank Prof. Hartmut Graßl who reviewed an early version of the manuscript and supervised the study. Special thanks to R. D. Susanto and Tien Sribimawati for providing Indonesian throughflow and some rainfall data, respectively. Calculations have been performed at the Deutsches Klimarechenzentrum (DKRZ).

References

Aldrian E, Susanto RD (2003) Identification of three dominant rainfall regions within Indonesia and their relationship to sea-surface temperature. Int J Climatol 23:1435–1452

Aldrian E, Gates LD, Widodo FH (2003) Variability of Indonesian rainfall and the Influence of ENSO and resolution in ECHAM4 simulations and in the reanalyses. MPI Report 346 (Available from Max Planck-Institut für Meteorologie, Bundesstr. 55, D-20146, Hamburg)

Aldrian E, Jacob D, Podzun R, Gates LD, Gunawan D (2004) Long term simulation of the Indonesian rainfall with the MPI Regional Model. Clim Dyn 22:795–814

Arakawa A, Lamb VR (1977) Computational design of the basic dynamical processes of the UCLA general circulation model. Methods Comput Phys 17:173–265

Berliand ME, Berliand TG (1952) Determining the net long-wave radiation of the earth with consideration of the efects of cloudiness. Isv Akad Nauk SSSR Ser Geo s 1:64–78

Budyko MI (1974) Climate and life in Int Geophys Ser, Academic, San Diago

Cressman GP (1959) An operational objective analysis scheme. Mon Weather Rev 117:765–783

Gibson JK, Kallberg P, Uppala S, Hernandez A, Nomura A, Serrano E (1997) The ECMWF Re-Analysis (ERA) 1. ERA Description. ECMWF Reanalysis Project Report Series 1 ECMWF, p 71 (Available from the European Centre for Medium-range Weather Forecasts, Reading)

Gordon AL, Susanto RD, Ffield A (1999) Throughflow within Makassar Strait. Geophys Res Lett 26:3325–3328

Hackert EC, Hastenrath S (1986) Mechanism of Java rainfall anomalies. Mon Weather Rev 114:745–757

Hendon HH (2003) Indonesian rainfall variability: Impacts of ENSO and local air-sea interaction. J Clim 16:1775–1790

Huffman GJ, Adler RF, Arkin P, Chang A, Ferraro R, Gruber A, Janowiak J, McNab A, Rudolf B, Schneider U (1997) The Global Precipitation Climatology Project (GPCP) combined precipitation data set. Bull Amer Meteor Soc 78:5–20

Jacob D (2001) A note to the simulation of the annual and inter-annual variability of the water budget over the Baltic Sea drainage basin. Met Atmos Phys 77:61–73

Jacob D, van den Hurk BJJM, Andræ U, Elgered G, Fortelius C, Graham LP, Jackson SD, Karstens U, Köpken C, Lindau R, Podzun R, Roeckel B, Rubel F, Sass BH, Smith RNB, Yang X (2001) A comprehensive model inter-comparison study investigation the water budget during the BALTEX-PIDCAP period. Met Atmos Phys 77:19–43

Jakob C (2000) The representation of cloud cover in atmospheric general circulation models. PhD Thesis Ludwig-Maximilians-Universitat, Munchen (Available from the European Centre for Medium-range Weather Forecasts, Reading) 190 pp

Kalnay E, Kanamitsu M, Kistler R, Collins W, Deaven D, Gandin L, Iredell M, Saha S, White G, Woollen J, Zhu Y, Chelliah M, Ebisuza W, Higgins W, Janowiak J, Mo KC, Ropelewski C, Wang J, Leetmaa A, Reynolds R, Jenne R, Joseph D (1996) The NCEP/NCAR 40-year reanalysis project. Bull Amer Meteor Soc 77:437– 471

Legutke S, Voss R (1999) The Hamburg atmosphere-ocean coupled circulation model ECHO-G. Technical Report 18 German Climate Computing Center Hamburg, p 61

Levitus S, Boyer TP, Conkright ME, O'Brien T, Antonov J, Stephens C, Stathoplos L, Johnson D, Gelfeld R (1998) World Ocean database 1998. In: Introduction. NOAA Atlas NESDIS 18, Ocean Climate Laboratory, National Oceanographic Data Center, Vol 1, US Government Printing Office, Washington

Majewski D (1991) The Europa Modell of the Deutscher Wetterdienst. In: ECMWF Seminar Proceedings ECMWF Reading, pp 147–191

Marsland SJ, Wolff JO (1998) East Antartic seasonal sea-ice and ocean stability: a model study. Ann Glaciol 27:477–482

Marsland SJ, Wolff JO (2001) On sensitivity of Southern Ocean sea ice to the surface fresh water flux: a model study. J Geophys Res 106:2723–2741

Marsland SJ, Haak H, Jungclaus JH, Latif M, Röske F (2003) The Max-Planck Institute global ocean/sea ice model with orthogonal curvilinear coordinates. Ocean Model 5:91–127

Meier HEM, Döscher R, Faxén T (2003) A multiprocessor coupled ice-ocean model for the Baltic Sea: application to salt inflow. J Geophys Res 108:C8–3273

Nicholls N (1979) A simple air-sea interaction model. Quart J Roy Meteor Soc 105:93–105

Peterson TC, Vose R, Schmoyer R, Razuvaev V (1998) Global Historical Climatology Network (GHCN) quality control of monthly temperature data. Int J Climatol 18:1169–1179

Press WH, Flannery BP, Teukolsky SA, Vetterling WT (1996) Numerical recipes in C Vol. 2 Cambridge University Press, Cambridge, p 963

Rayner NA, Horton EB, Parker DE, Folland CK, Hackett RB (1996) Version 2.2 of the global sea-ice and sea-surface temperature data set, 1903-1994. Technical Note CRTN74. Clim Res p 35

Roeckner E, Arpe K, Bengston L, Christoph M, Claussen M, Dumenil L, Esch M, Giorgetta M, Schlese U, Schulzweida U (1996) The atmospheric general circulation model ECHAM-4: Model description and simulation of present-day climate. MPI Report 218, p 90 (Available from Max Planck-Institut für Meteorologie, Bundesstr. 55, D-20146, Hamburg)

Röske F (2001) An Atlas of surface fluxes based on the ECMWF Re-Analysis: a climatological dataset to force global ocean general circulation models. MPI Report 323 (Available from Max Planck-Institut für Meteorologie, Bundesstr. 55, D-20146, Hamburg)

Schrum C, Hubner U, Jacob D, Podzun R (2003) A coupled atmosphere/ice/ocean model for the North Sea and the Baltic Sea. Clim Dyn 21:131–151

Simmons AJ, Gibson JK (2000) The ERA-40 Project Plan. ERA-40 Project Report Series 1 ECMWF, p 62 (Available from the European Centre for Medium-range Weather Forecasts, Reading)

Terray L, Valcke S, Piacentini A (1999) OASIS 2.3 Ocean atmosphere sea ice soil user's guide. Technical Report TR/CGMC/99-37 CERFACS p 82

Valcke S, Terray L, Piacentini A (2000) The OASIS Coupler User's Guide, Version 2.4. Technical Report TR/CGMC/00-10 CERFACS, p 85

Vose RS, Schmoyer RL, Steurer PM, Peterson TC, Heim R, Karl TR, Eischeid JK (1992) The Global Historical Climatology Network: Long-term monthly temperature, precipitation, sea level pressure, and station pressure data. ORNL/CDIAC-53 NDP-041 p 325

Wolff JO, Maier-Reimer E, Legutke S (1997) The Hamburg Ocean Primitive Equation Model HOPE. Technical Report 13 German Climate Computer Center (DKRZ) Hamburg, p 98